BJP British Journal of Pharmacology

DOI:10.1111/bph.12104
www.brjpharmacol.org

RESEARCH PAPER

MPP+-dependent inhibition of I_h reduces spontaneous activity and enhances EPSP summation in nigral dopamine neurons

A Masi*, R Narducci*, E Landucci, F Moroni and G Mannaioni

Department of Neurosciences, Psychology, Drug Research and Child Health – Section of Pharmacology and Toxicology, University of Florence, Florence, Italy

Correspondence
Alessio Masi, Department of Neurosciences, Psychology, Drug Research and Child Health – Section of Pharmacology and Toxicology, University of Florence, Viale G. Pieraccini 6, 50139 Firenze, Italy. E-mail: alessio.masi@unifi.it

*These authors contributed equally.

Keywords
MPP+; MPTP; Parkinson's disease; dopamine neurons; I_h; HCN channels; synaptic summation

Received
10 July 2012
Revised
21 December 2012
Accepted
7 January 2013

BACKGROUND AND PURPOSE

1-Methyl-4-phenylpyridinium (MPP+), a potent parkinsonizing agent in primates and rodents, is a blocker of mitochondrial complex I, therefore MPP+-induced parkinsonism is believed to depend largely on mitochondrial impairment. However, it has recently been proposed that other mechanisms may participate in MPP+-induced toxicity. We tackled this issue by probing the effects of an acute application of MPP+ on *substantia nigra pars compacta* (SNc) dopamine (DA) neurons.

EXPERIMENTAL APPROACH

The effects of MPP+ on SNc DA neurons in acute midbrain slices were investigated with electrophysiology techniques.

KEY RESULTS

MPP+ (50 μM) was able to (i) hyperpolarize SNc DA neurons by ~6 mV; (ii) cause an abrupt and marked (over 50%) reduction of the spontaneous activity; and (iii) inhibit the hyperpolarization-activated inward current (I_h). MPP+ shifted I_h activation curve towards negative potentials by ~11 mV both in Wistar rats and in C57/BL6 mice. Inhibition was voltage- and concentration-dependent (I_{max} = 47%, IC_{50} = 7.74 μM). MPP+ slowed I_h activation kinetics at all potentials. These effects were not dependent on (i) block of mitochondrial complex I/fall of ATP levels; (ii) activation of type 2 DA receptor; and (iii) alteration of cAMP metabolism. Finally, MPP+-dependent inhibition of I_h facilitated temporal summation of evoked EPSPs in SNc DA, but not in CA1 hippocampal neurons.

CONCLUSION AND IMPLICATIONS

Reduced functionality of I_h in SNc DA neurons, via increased responsiveness towards synaptic excitation, might play a role in MPP+-induced parkinsonism and, possibly, in the pathogenesis of human Parkinson's.

Abbreviations

Ca_v 1.3, voltage-gated calcium channels 1.3; D_2R, type 2 dopamine receptor; DA, dopamine; DAT, dopamine transporter; eEPSP, evoked EPSP; HCN, hyperpolarization-activated cyclic nucleotide-gated channels; I_h, hyperpolarization-activated inward current; K_{ATP}, ATP-sensitive K^+ channels; MPP^+, 1-methyl-4-phenylpyridinium; MPTP, 1-methyl-4-phenyl-1,2,3,6-tetrahydropyridine; PD, Parkinson's disease; PIP_2, phosphatidylinositol 4,5-bisphosphate; PS, parkinsionian syndrome; ROS, reactive oxygen species; SNc, *substantia nigra pars compacta*; STN, sub-thalamic nucleus

Introduction

1-Methyl-4-phenylpyridinium (MPP^+) is a neurotoxin able to induce a parkinsonian syndrome in experimental animals, following intra-nigral administration or enzymatic conversion of the pro-toxin 1-methyl-4-phenyl-1,2,3,6-tetrahydropyridine (MPTP). As a lipophilic molecule, MPTP readily crosses the blood–brain barrier after systemic injection. Once in the brain, MPTP is converted into MPP^+ by MAO-B in glial cells. MPP^+ is then selectively uptaken by dopaminergic neurons through the dopamine (DA) transporter (DAT; Fuller and Hemrick-Luecke, 1985; Irwin and

Langston, 1985). Here, MPP+ accumulates in mitochondria where it inhibits complex I, leading to ATP depletion, oxidative stress and, eventually, neuronal death (Smeyne and Jackson-Lewis, 2005). In the mouse, MPP+ intoxication leads to severe nigro-striatal degeneration and up to 90% depletion of striatal DA (Jackson-Lewis and Przedborski, 2007). In rats, MAO-B activity is low, therefore *substantia nigra pars compacta* (SNc) DA degeneration is only observed after intra-nigral injection of the active metabolite MPP+ (Heikkila *et al.*, 1985; Blandini and Armentero, 2012; Lin *et al.*, 2012). The discovery of the parkinsonizing action of MPP+ has laid the foundation for the theory that mitochondrial impairment and elevation of oxidative stress is pivotal in Parkinson's disease (PD) pathogenesis (Greenamyre *et al.*, 1999). Recently, however, results have been presented that challenge this theory. One group has reported that vulnerability to MPP+ is retained in midbrain DA neurons isolated from mice carrying a defective complex I (Choi *et al.*, 2008). Furthermore, MPP+ has been shown to affect synaptic activity in hippocampal slices and cultured midbrain neurons (Galvan *et al.*, 1987; Lee *et al.*, 2008). In SNc DA neurons, perforated patch recordings have shown that acute application of MPP+ leads to the opening of K_{ATP} due to block of complex I and depletion of cellular ATP (Liss *et al.*, 2005). We focused our attention on acute actions of MPP+ that are *not* related to mitochondrial failure and ATP depletion. To this aim, we challenged rat SNc DA neurons with relevant concentrations of MPP+ and performed whole-cell/cell-attached recordings. We found that MPP+, at concentrations approaching those used to induce nigrostriatal degeneration in mice (Jackson-Lewis and Przedborski, 2007) and rats (Lin *et al.*, 2012), hyperpolarizes the cell membrane and reduces the spontaneous firing of SNc DA neurons. This effect occurs under blockade of K_{ATP} channels and in the presence of 2 mM ATP (in whole-cell solution). This effect is accompanied by the inhibition of hyperpolarization-activated inward current (I_h), an inward-rectifying, non-inactivating cationic current found in many brain areas and implicated in several physiological and pathological processes (Biel *et al.*, 2009). The inhibitory effect of MPP+ on I_h is voltage-dependent and affects both current amplitude at the steady-state and gating kinetics. Pharmacological experiments indicate that none of the expected pathways (complex I impairment, DA and cAMP signalling) are involved, thus suggesting a direct interaction with the channel complex. Finally, we found that MPP+ enhanced temporal summation of evoked EPSPs (eEPSPs) in SNc DA neurons, but not in CA1 neurons.

Methods

Preparation of rat midbrain slices and electrophysiology

Animals were purchased from Harlan Italia (Milan, Italy). Housing, handling and killing were in compliance with the European and Italian legislation (DL 116/92). All studies involving animals are reported in accordance with the ARRIVE guidelines for reporting experiments involving animals (Kilkenny *et al.*, 2010; McGrath *et al.*, 2010). Juvenile (2–3 weeks, $n = 89$), adult (8 weeks, $n = 5$) Wistar Han rats and C57/BL6 mice (8 weeks, $n = 8$) were used. Unless otherwise specified, experiments were performed with preparations obtained from juvenile rats. Animals were killed by decapitation under anaesthesia with isoflurane. Brains were removed and mounted in the slicing chamber of a vibroslicer (Leica VT 1000S, Leica Microsystems, Wetzlar, Germany). Horizontal slices (250 µm in thickness) were cut from midbrain and hippocampi in chilled artificial CSF (aCSF) saturated with 95% O_2/5% CO_2 containing (in mM) 130 NaCl, 3.5 KCl, 1.25 NaH_2PO_4, 25 $NaHCO_3$, 10 glucose, 2 $CaCl_2$ and 2 $MgSO_4$. Slices were allowed to recover in the same solution maintained at 34°C with constant oxygenation for 1 h prior to experiments. The recording chamber was mounted on an upright microscope (Nikon Eclipse E600 FN, Nikon Corporation, Tokyo, Japan) equipped with infrared-differential interference contrast optics and an infrared camera (Hamamatsu, Arese, Italy) for visually guided experiments. Once positioned in the recording chamber, slices were bathed with oxygenated aCSF maintained at 33–34°C with a TC344B temperature controller (Warner, Handen, CT, USA). Flow rate was 1 mL/min and driven by gravity. Solution exchange was achieved with a remote-controlled Hamilton MVP line switch (Hamilton Bonaduz AG, Bonaduz, Switzerland). Patch pipettes were made from thin-walled borosilicate capillaries (Harvard Apparatus, London, UK) with a vertical puller (Narishige PP830, Narishige International Ltd, London, UK) and back-filled with an intracellular solution containing (in mM) K^+ gluconate (120), KCl (15), HEPES (10), EGTA (5), $MgCl_2$, (2), Na_2PhosphoCreatine (5), Na_2GTP (0.3), MgATP (2), resulting in a resistance of 3–4 MΩ in the bath. This solution was used for both cell-attached and whole-cell recordings. During whole-cell voltage clamp recordings access resistance was monitored throughout experiments with short, –10 mV steps. Recordings undergoing a variation in access resistance ≥10% were discarded. No whole-cell compensation was used. Signals were sampled at 10 kHz, low-pass filtered at 3 kHz, acquired with an Axon Multiclamp 700B and digitized with a Digidata 1440 A and Clampex 10 (Axon, Sunnyvale, CA, USA). For the analysis of the effect on firing rate and potential, average values were calculated from 30 s frames immediately before and after 5 or 10 min of application of, respectively, MPP+ and ZD7288. For recordings of eEPSPs in SNc, a tungsten bi-polar stimulation electrode (FHC, Bowdoin, ME, USA) was placed in proximity of the subthalamic nucleus (STN) and used to deliver trains of depolarizing stimuli (pulse frequency = 20 Hz, duration = 20 µs, amplitude = 5–15 mV) generated with a computer-controlled isolated stimulator (Digitimer, Welwyn Garden City, UK). In the hippocampus, stimulation electrode was inserted in the *stratum radiatum* and used to elicit eEPSPs in CA1 pyramidal neurons as described for the SNc. Membrane potential was maintained at –55 to –60 mV (SNc) or –65 to –70 mV (CA1) by injecting negative current, to prevent the firing of action potentials during eEPSP trains. eEPSPs were generated under pharmacological block of NMDA and $GABA_A$ receptors with, respectively, D-AP5 50 µM and gabazine 10 µM. During summation experiments, I_h was elicited with negative voltage steps (–20 mV) from –55 mV (SNc) and –65 mV (CA1).

Data analysis and statistics

Pooled data throughout the paper are presented as mean ± SEM of 'n' independent experiments. Unless otherwise speci-

fied, statistical difference between means is assessed with a Student *t*-test for paired samples (Origin 8.1 and Graphpad Prism, Microcal, Northampton MA, USA/ La Jolla, CA, USA). Significance at the $P < 0.05$, 0.01, 0.001 and 0.0001 level is indicated with *, **, ***, ****, respectively in figures. When single recordings are shown, they are intended to represent typical observations. Capacitance transients occurring during voltage steps, never compensated for during recordings, were graphically removed from all traces displayed in figures. Holding current was measured at –55 mV, while input resistance was determined with short (200 ms), –10 mV steps from holding. For activation curves, tail currents at –135 mV were normalized, plotted against pre-pulse potential (–45 to –135 mV) and fitted with a Boltzmann equation: $y = A_2 + (A_1 - A_2)/(1 + e^{(x-x0)\times dx})$. For the concentration–inhibition curve, the effect of MPP$^+$ on I_h elicited at –75 mV was plotted against concentration (1–100 μM). The fitting curve was obtained with a Logistic equation: $y = A_2 + (A_1 - A_2)/1 + (x - x_0)^p$. To quantify the effect of MPP$^+$ on the kinetic properties of I_h, currents elicited at –95, –115 and –135 mV were fitted with a double exponential: $y = y_0 + A_1 \times e^{-x/t1} + A_2 \times e^{-x/t2}$. The same equation was used to fit depolarization after the sag elicited with –200 pA current steps. The ratio eEPSP 5/eEPSP 1 was considered to compare temporal summation in control, MPP$^+$ and MPP$^+$ + ZD7288. To avoid biases, recordings were only included in the analysis when the amplitude of eEPSP 1 was stable. Traces in Figure 7 were baseline-adjusted to appreciate changes in summation. Graphs, histograms and fittings were generated in Origin 8.1.

Drugs and chemicals

All drugs were bath-applied unless otherwise indicated. MPP$^+$ iodide (Sigma, Milan, Italy) was dissolved in water to 100 mM and used at 1–100 μM. Other drugs used were: ZD7288 [Tocris, 100 mM in water, used at 30 μM; Bristol, UK); rotenone (Sigma, 10 mM in dimethylsulfoxide (DMSO), used at 1 μM]; glybenclamide (Sigma, 100 mM in DMSO, used at 10 μM); GBR12783 (Tocris, 5 mM in water, used at 5 μM); sulpiride (Sigma, 10 mM in ethanol, used at 10 μM); D-AP5 (Abcam, 100 mM in water, used at 50 μM; Abcam Biochemicals, Bristol, UK); gabazine (Abcam, 10 mM in water, used at 10 μM); cAMP (Sigma, 100 mM in water, used at 100 μM in pipette solution); IBMX (Sigma, 50 mM in DMSO, used at 1 mM in pipette solution with cAMP). cAMP was allowed to diffuse for 5 min before MPP$^+$ application.

Results

MPP$^+$ causes rapid, ATP-independent, hyperpolarization and reduction of spontaneous activity in SNc DA neurons

SNc DA neurons were identified on the basis of their morphology (Figure 1A) and electrophysiological profile (Figure 1B–D). Typical DA neurons display slow (2–3 Hz) and regular autonomous firing activity (Figure 1B), and a rebound potential (sag) in response to hyperpolarizing current pulses (Figure 1C). In voltage clamp, a family of slow-activating,

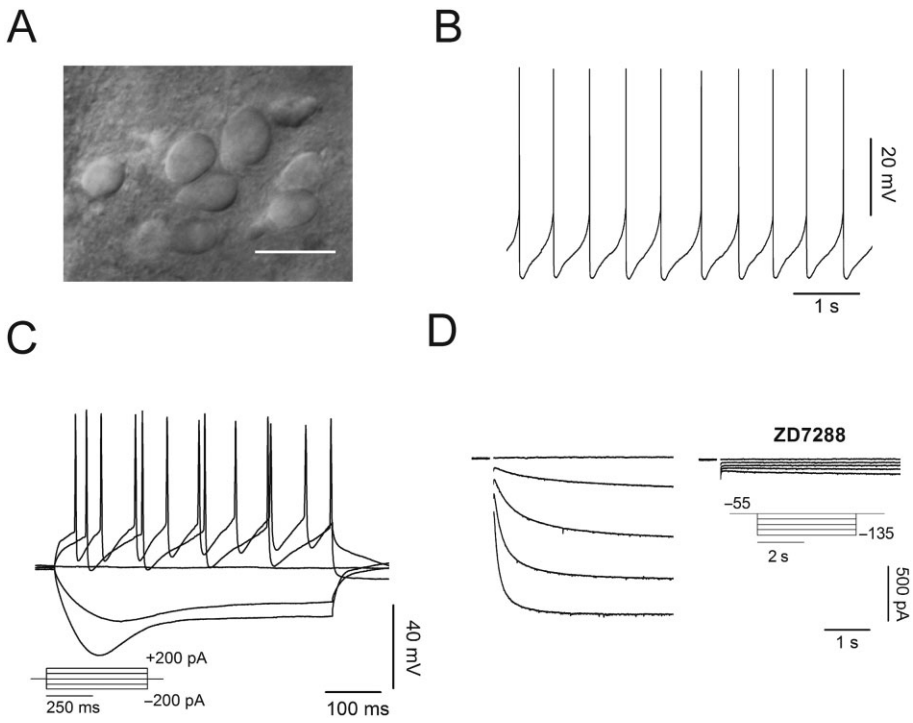

Figure 1

Identification of putative SNc DA neurons within SNc in rat midbrain slices. (A) Infrared image of a microscopic field showing DA neurons (scale bar = 20 μm). (B, C) Whole-cell voltage recordings showing typical electrophysiological features of SNc DA neurons: slow and regular pace making (B) and a pronounced rebound depolarization following injection of negative current (C). (D) Currents elicited with 4 s hyperpolarizing voltage steps from –55 (V_{HOLD}) to –135 mV in 20 mV increments. These currents are fully abolished by I_h organic blocker ZD7288 (30 μM).

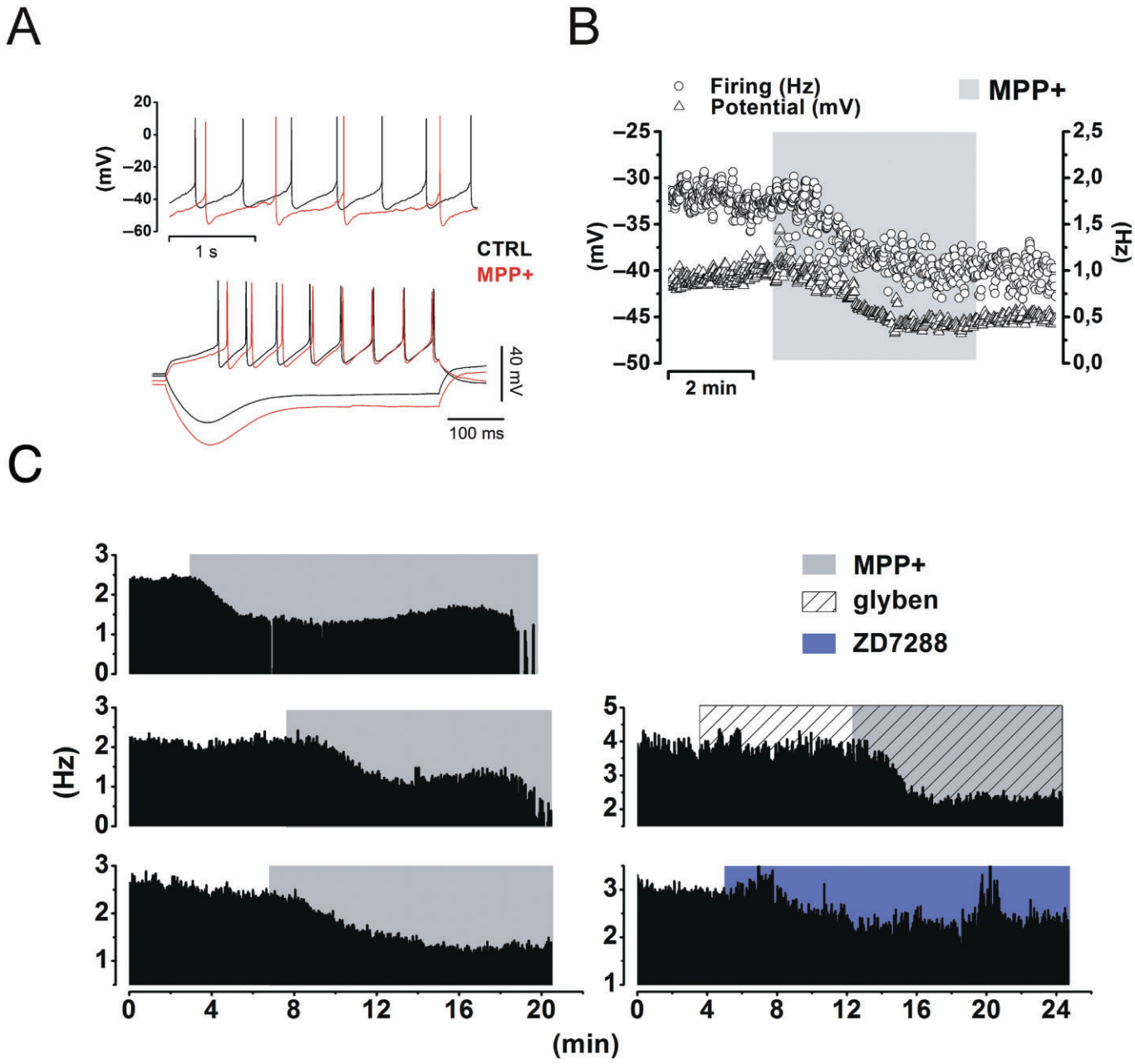

Figure 2

MPP+ produces a rapid, K_{ATP} channel-independent hyperpolarization and reduction of the firing rate in SNc DA neurons. (A) Top, illustrative whole-cell current clamp recording from an SNc DA neuron before (black) and after (red) 5 min of bath application of MPP+ 50 μM. The cell membrane is hyperpolarized (–55.28 ± 3.46 mV vs. –61.99 ± 3.5 mV, $n = 8$, $P = 0.002$) and firing rate reduced (2.13 ± 0.12 Hz to 0.9 ± 0.14 Hz, $n = 13$, $P = 7.8 \times 10^{-7}$). Bottom, voltage response to negative (–200 pA) and positive (+200 pA) currents. Note the hyperpolarization, the increase in sag amplitude and the longer time to first peak. (B) Time course of the action of MPP+ on firing frequency and membrane potential. Note the fast kinetics of the effect. (C) Cell-attached recordings of three SNc DA neurons showing the rapid drop in firing rate followed by delayed silencing of spontaneous activity produced by MPP+ (50 μM, left). The cessation of electrical activity is often gradual (top, middle). The rapid effect is not prevented by pre-incubation with glybenclamide (10 μM), a selective blocker of K_{ATP} channels (2.34 ± 0.48 Hz vs. 1.18 ± 0.71 Hz, $n = 5$, $P = 0.006$, right, middle). Finally, selective inhibition of I_h with the organic blocker ZD7288 (30 μM) mimics the effect of MPP+, although with slower kinetics (2.18 ± 0.31 Hz vs. 1.5 ± 0.25 Hz, $n = 4$, $P = 0.017$, right bottom).

inward relaxations (I_h) develop in response to hyperpolarizing potentials (Figure 1D). Such currents are fully abolished by 30 μM ZD7288, a selective organic blocker of I_h. Neurons with such properties were challenged with MPP+ 50 μM in bath application and recorded in whole-cell and cell-attached configurations (Figure 2). This concentration was chosen on the basis of midbrain levels of MPP+ detected by HPLC after a standard MPTP injection schedule of experiments *in vivo*

(Jackson-Lewis and Przedborski, 2007). In presence of MPP^+ 50 μM the spike rate of spontaneously firing cells dropped from 2.13 ± 0.12 Hz to 0.9 ± 0.14 Hz, (–58 ± 0.9%, $n = 13$, $P = 7.8 \times 10^{-7}$, Figure 2A, B). In addition to a reduction of the firing rate, a substantial shift of the membrane potential towards negative values (measured from current clamp signatures as shown in Figure 2A) was observed (–55.28 ± 3.46 mV vs. –61.99 ± 3.5 mV, $n = 8$, $P = 0.002$, Figure 2A, B). These effects were normally rapid (see time scale bar in Figure 2B) coming to completion in 5 min. A series of other parameters were measured, in control conditions and in presence of MPP^+, from current clamp protocols as the one shown in Figure 2A (bottom): firing threshold, rate of rise, action potential amplitude, sag amplitude and after-sag depolarization kinetics. These values are summarized in Table 1. To test the effect of longer MPP^+ incubation, we used cell-attached recordings, in which the integrity of cell membrane and intracellular fluid are preserved (Figure 2C). In line with whole-cell recordings, the effect of MPP^+ reached a first plateau within the first 5 min of application. Afterwards, after 15–20 min of continuous application, silencing of spontaneous activity was generally observed, as shown for three examples (Figure 2C, left). The inhibition of spontaneous firing of SNc DA upon acute administration of MPP^+ was described before and explained as a consequence of complex I impairment and ensuing fall of cellular ATP levels (Liss *et al.*, 2005). Reduced ATP levels lead to activation of K_{ATP} channels, membrane hyperpolarization and, eventually, cessation of firing activity. On these premises, we tested the involvement of K_{ATP} channels on the early effects of MPP^+ application. Pre-incubation with the K_{ATP} blocker glybenclamide (10 μM) did not prevent, or dampen, the rapid drop in firing rate (2.34 ± 0.48 Hz vs. 1.18 ± 0.71 Hz, $n = 5$, $P = 0.006$, Figure 2C, right). On the other hand, application of 30 μM ZD7288 induced a decay of firing activity, similar in extent to that induced by MPP^+ (2.18 ± 0.31 Hz vs. 1.5 ± 0.25 Hz, –31 ± 20%, $n = 4$, $P = 0.017$ vs. control, $P = 0.28$ vs. MPP^+, Figure 2C, right).

Table 1

Changes in electropyshiological parameters of SNc DA neurons induced by MPP^+ 50 μM

		CTRL	MPP^+	*n, p*
I_{HOLD} (pA)		–59.54 ± 33.25	–30.18 ± 39.36	11, 0.005
R_{in} (MΩ)		222.15 ± 21.14	343.65 ± 41.75	11, 0.003
Threshold (mV)		–33,93 ± 0,96	–34,34 ± 0,87	9, 0.685
Spike amp. (mV)		56,72 ± 2,68	58,08 ± 2,43	8, 0.082
Rate of rise (mV/ms)		188,71 ± 51,06	216,08 ± 49,58	8, 0.317
SAG (mV)		39,28 ± 11,30	42,20 ± 11,73	8, 0.404
SAG after depol.	t_1	47,27 ± 9,95	88,21 ± 25,46	8, 0.133
	t_2	62,46 ± 12,57	80,63 ± 20,56	8, 0.450

MPP^+ inhibits I_h by slowing its gating properties and reducing current amplitude

Previous reports have shown that pharmacological block of I_h reduces the firing rate of SNc DA neurons (Seutin *et al.*, 2001; Zolles *et al.*, 2006; Inyushin *et al.*, 2010). On this basis, we tested whether the rapid action of MPP^+ on firing frequency of SNc DA neurons could depend on modulation of I_h. To this purpose, we performed whole-cell voltage clamp recordings. Consistently with the closing of an inward, cationic current, partially available at the imposed holding potential (–55 mV), application of 50 μM MPP^+, caused a modest upward shift of the holding current (–59.54 ± 33.25 pA to –30.18 ± 39.36 pA, $n = 11$, $P = 0.005$) and a rise of the input resistance (222.15 ± 21.14 MΩ to 343.65 ± 41.75 MΩ, $n = 11$, $P = 0.003$). We then studied how MPP^+ affects I_h activation curve. We used a double-phase voltage clamp protocol in which a family of conditioning potentials (–45 mV to –135 mV, 4 s in duration, holding = –55 mV), are imposed, followed by a fully-activating pulse to –135 mV. With this protocol, traces as those in Figure 3A are obtained, before (left) and after (right) 5 min of incubation with 50 μM MPP^+. Normalized tail currents at –135 mV (magnifications) were analysed and plotted to obtain activation curves as in Figure 3B, C and D. In juvenile rats, $V_{1/2}$ was shifted from –76.29 ± 1.50 mV to –88.26 ± 1.59 mV ($n = 8$, $P = 0.001$) by 5 min of MPP^+. For control, the same experiment was repeated in SNc DA neurons from 8-week-old Wistar rats or 8-week-old C57/BL6 male mice, the latter being the animal model of choice in MPTP studies. In adult rats, MPP^+ shifted $V_{1/2}$ from –82.44 ± 1.43 mV to –90.73 ± 2.5 mV ($n = 7$, $P = 0.011$), in mice, from –76.1 ± 2.13 mV to –87.88 ± 2.31 mV ($n = 7$, $P = 0.002$). MPP^+-dependent $V_{1/2}$ shift was quantitatively similar in the three groups (juvenile rats vs. adult rats, $P = 0.62$; juvenile rats vs. mice, $P > 0.99$ and adult rats vs. mice $P = 0.85$, one-way ANOVA followed by Bonferroni *post hoc* analysis) ruling out the possibility of species- or age-related variability of the observed effect. Next, we studied in depth the voltage-dependence of the effect of MPP^+ on steady state current with a double-pulse (–75/–135 mV) stimulation protocol (Figure 4A). As shown, steady state current reduction (black arrow in insets) is marked at –75 mV (–44.38 ± 7.39%, $n = 8$, $P = 5.4 \times 10^{-4}$), while nearly absent at –135 mV (–5 ± 5.4%, $n = 8$, $P = 0.4$). A concentration/inhibition curve was obtained by plotting the percentage of inhibition at –75 mV, obtained with the two-step voltage clamp protocol described earlier, versus MPP^+ concentration ($I_{max} = 47\%$; $IC_{50} = 7{,}74$ μM, Figure 4B).

MPP^+ changes the kinetic properties of I_h

Data reported in Figures 3 and 4 indicate that MPP^+-dependent inhibition of I_h shows a peculiar voltage dependence. Indeed, as the imposed potential becomes more hyperpolarized, the effect of MPP^+ on current amplitude at steady-state decreases, eventually approaching zero at –135 mV. Nevertheless, a sizeable alteration of the activation

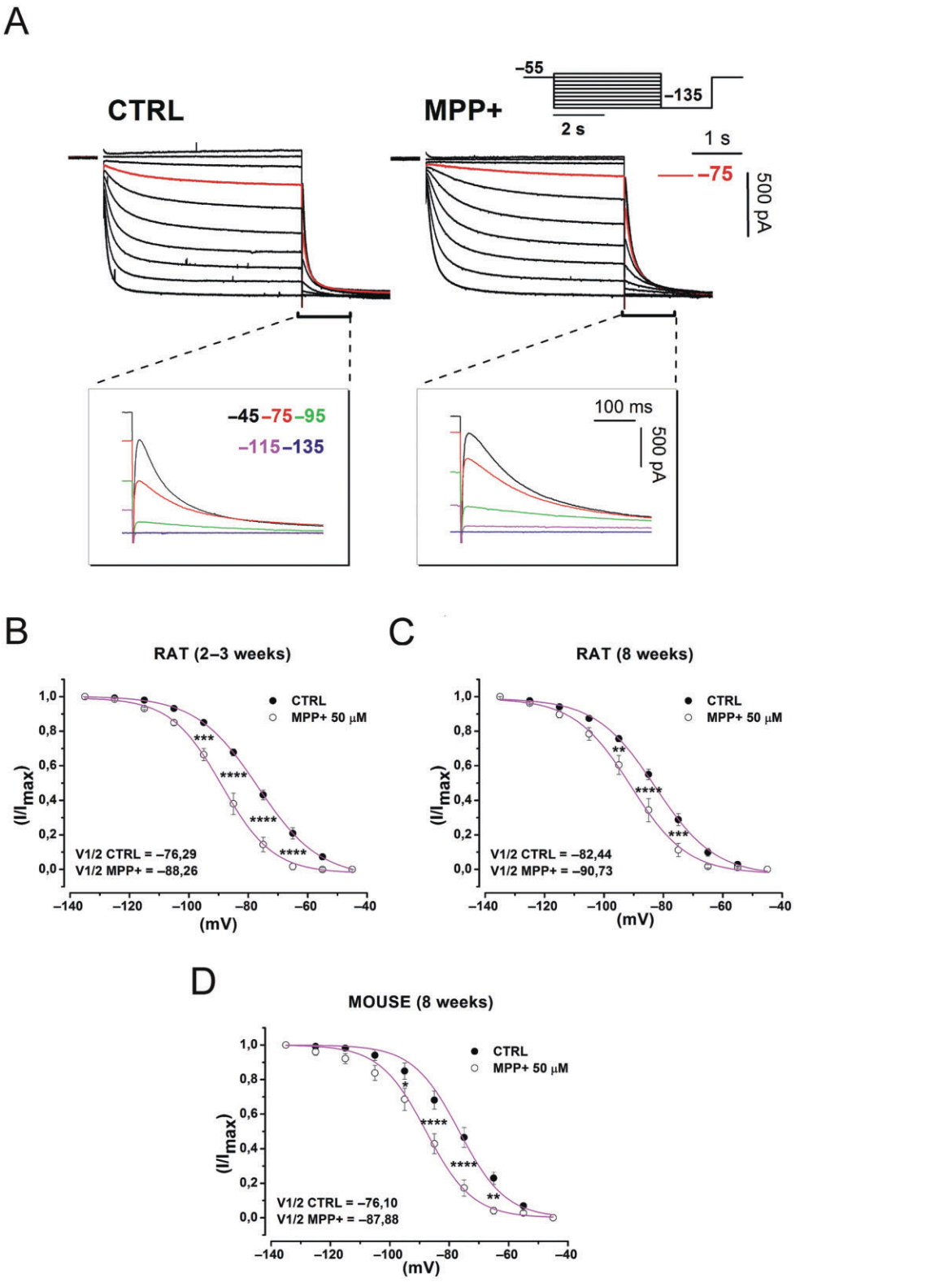

Figure 3

MPP+ changes the voltage dependence of I_h. (A) Whole-cell currents elicited with a family of hyperpolarizing potentials (scheme). Currents evoked at –75 mV are highlighted in red. Enlargements show tail currents obtained at the indicated potentials. (B, C, D) I_h activation curve obtained by plotting normalized tail currents versus potential in control conditions (closed circles) and MPP+ 50 µM (open circles) in SNc DA neurons from juvenile rats (B), adult rats (C) and C57/BL6 male mice (D). *P*-values were obtained with one-way ANOVA with Bonferroni *post hoc* analysis. Curves were fitted with a Boltzmann equation. CTRL, control.

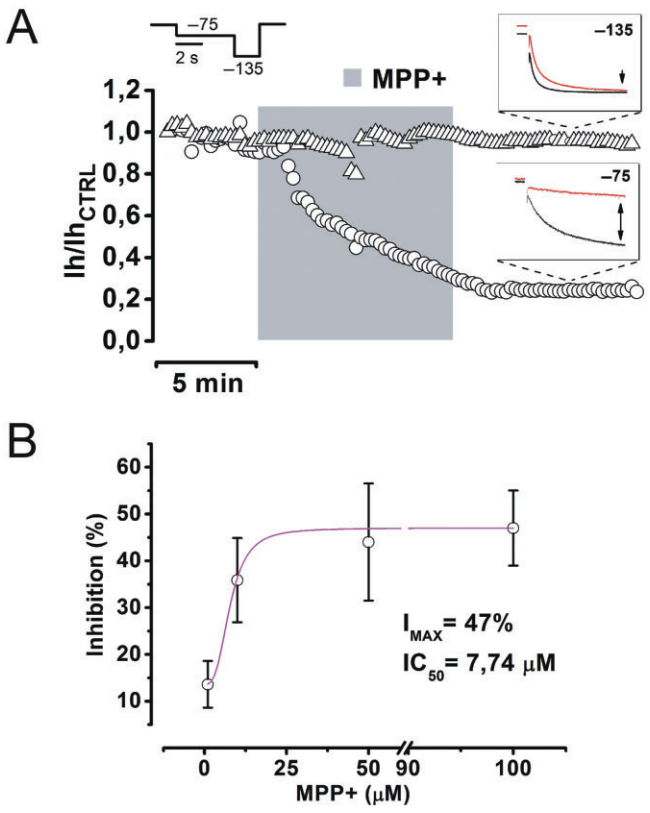

Figure 4

MPP+ inhibits I_h in a voltage- and concentration-dependent manner. (A) A time course of the effect of MPP+ 50 µM on I_h at –75 (circles) and –135 mV (triangles) was obtained with the double-pulse protocol shown above. Insets show typical currents evoked before (black) and after (red) MPP+ (–75 mV = –44.38 ± 7.39%, n = 8, P = 5.4 × 10^{-4}; –135 mV = –5 ± 5.4%, n = 8, P = 0.4. (B) Concentration-inhibition curve obtained by fitting values of inhibition (in percentage of control) at –75 mV, in presence of 1 (n = 5), 10 (n = 5), 50 (n = 5) and 100 µM MPP+ (n = 6). Values of I_{MAX} (47%) and IC_{50} (7.74 µM) were obtained by fitting the curve with a logistic equation (Methods).

kinetics of I_h is present at all potentials, becoming most evident at the most negative ones. This action was quantified by fitting inward currents elicited at –95, –115 and –135 mV with a double exponential decay function (Franz *et al.*, 2000), in control conditions and in presence of MPP+ 50 µM (Figure 5A). This equation fitted all traces under analysis with an $R^2 \geq 0.99$. MPP+ increases t_{FAST} and t_{SLOW} by approximately twofold at –95 mV (P = 0.026 and P = 0.047 vs. pre-MPP+, n = 8), by 50% at –115 mV (P = 0.003 and P = 0.01, n = 8) and –135 mV (P = 0.0015 and P = 0.004, n = 8).

Effect of MPP+ on I_h does not depend on complex I poisoning, type 2 dopamine receptor (D_2R) signalling or cAMP metabolism

To further investigate the inhibitory action of MPP+ on I_h, we tested the involvement of pathways that, according to several reports, may provide mechanistic insight for this phenomenon (Figure 6). We first tested whether the effect of MPP+ on

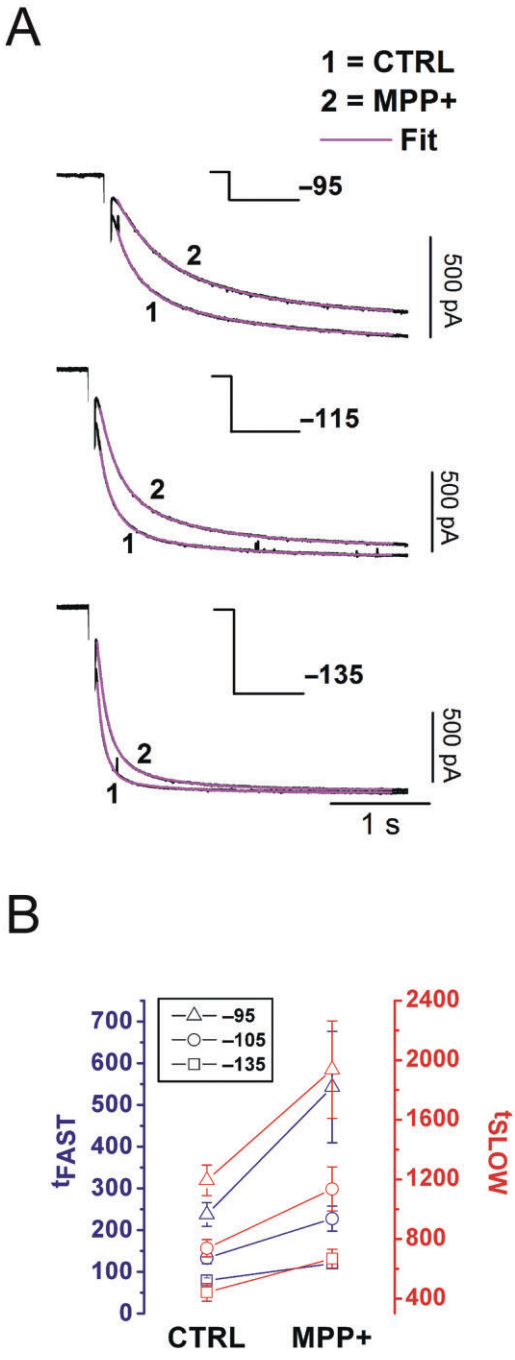

Figure 5

MPP+ alters the activation kinetics of I_h in a voltage-dependent manner. (A) I_h currents elicited at –95, –115 and –135 mV evoked in control and after MPP+ 50 µM are shown. Fits are shown in magenta. Stimulation protocol is indicated in each panel. (B) Effect of MPP+ on t_{FAST} (blue) and t_{SLOW} (red) obtained at –95 (triangle), –115 (circle) and –135 mV (square) in control conditions and in MPP+ (n = 8). CTRL, control.

I_h was downstream of complex I blockade. We have already shown that activation of K_{ATP} channels is not responsible for the effects on spontaneous activity, as these occur in presence of ATP and are not prevented by K_{ATP} blocker glybenclamide.

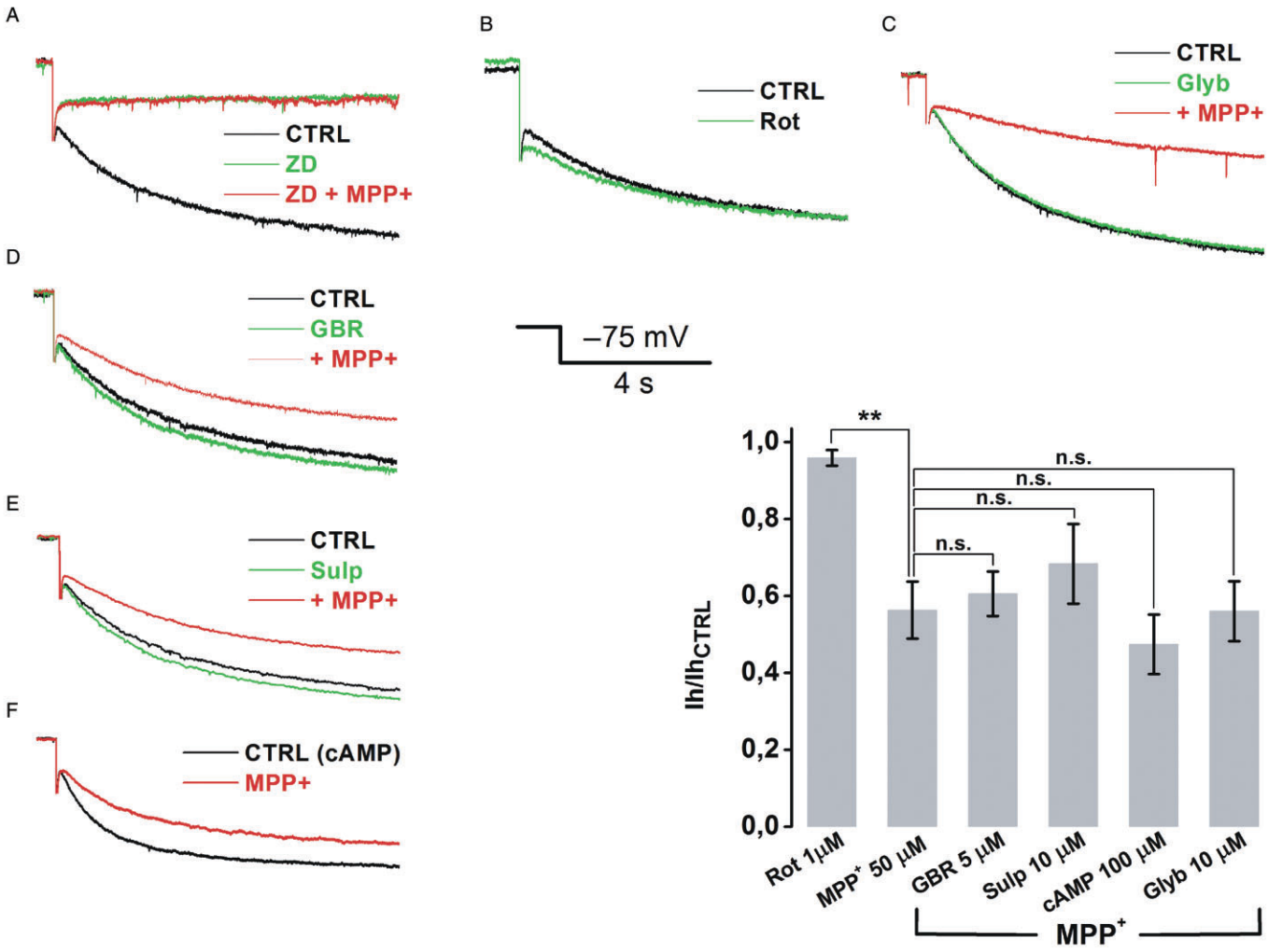

Figure 6

MPP+-inhibition of I_h in SNc DA neurons does not involve mitochondrial or cAMP metabolism. Representative traces for each pharmacological experiment in which drugs were tested for their ability to mimic/prevent the action of MPP+ 50 µM on steady-state I_h elicited with single, 4 s pulses to –75 mV (Figure 6A–F). ZD7288 30 µM completely occluded the action of MPP+ (A). Rotenone 1 µM did not affect I_h, (n = 5, P > 0.99, B). Consistently, 10 µM glybenclamide did not protect I_h from MPP+ inhibition (n = 5, P > 0.99, C). DAT blocker GBR12738 (5 µM, n = 8, P > 0.99, D), D_2R antagonist sulpiride (10 µM, n = 5, P > 0.99, E) and cAMP 100 µM added to pipette solution (+ IBMX 1 mM, n = 4, P > 0.99, F), failed to prevent the inhibition caused by MPP+ 50 µM. Grouped data and statistical analysis from pharmacology experiments. Statistical difference between each group and MPP+ was calculated with one-way ANOVA with Bonferroni *post hoc* analysis. CTRL, control.

As for I_h inhibition, it has been published that rotenone, a pesticide and complex I blocker, is able to open K_{ATP} channels, with an ATP-independent, reactive oxygen species- (ROS) dependent mechanism (Freestone *et al.*, 2009). In turn, the opening of potassium channels active at near-rest potentials has been associated to reduced space-clamp and apparent reduction of I_h (Cathala and Paupardin-Tritsch, 1999). To rule out this possibility, we applied rotenone 1 µM to SNc DA neurons while eliciting I_h with 4 s pulses to –75 mV (V_{HOLD} = –55 mV), every 15 s. No significant effect on I_h amplitude was observed (95.96 ± 2%, n = 5, P > 0.99; MPP+ = 43.7 ± 7.43%, n = 8, P = 0.0128; rotenone vs. MPP+, P = 0.004, Figure 6B). In addition, block of K_{ATP} channels with a pre-incubation with 10 µM glybenclamide failed to prevent MPP+-induced inhibition of I_h, (44 ± 7.8%, n = 4, P > 0.99 vs. MPP+ alone, Figure 6C), providing further evidence that I_h reduction is not secondary to changes in whole-cell parameters, such as reduced clamp, due to opening of K_{ATP}. We then assessed the role of DAT, responsible for selective MPP+ accumulation in SNc DA neurons (Fuller and Hemrick-Luecke, 1985). Application of MPP+ 50 µM following a 10 min pre-incubation with the specific blocker GBR12783 (5 µM) reduced I_h to an extent similar to MPP+ alone (39.44 ± 5.79%, n = 4, P > 0.99 vs. MPP+, Figure 6D). Next, the hypothesis that MPP+ could inhibit I_h by mimicking the action of DA on DA receptors was tested. Several laboratories have observed that activation of DA receptors on midbrain DA neurons induces effects reminiscent of those described here, namely hyperpolarization of the membrane potential, slowing of firing rate (Lacey *et al.*, 1987) and down-modulation of I_h (Jiang *et al.*, 1993; Cathala and

Paupardin-Tritsch, 1999; Vargas and Lucero, 1999). These effects have been attributed to activation of D_2Rs, which inhibit adenylate cyclase and reduce cAMP levels thereby modulating a number of ion channels, such as G-protein-gated inward rectifying K^+ channels and I_h. Given the well established pharmacological similarities between MPP^+ and DA we reasoned that MPP^+ may inhibit I_h through D_2R-mediated reduction of cAMP levels. However, pre-incubation with the D_2R-selective antagonist sulpiride (10 μM, 5 min) failed to prevent the effect of 50 μM MPP^+ (31.63 ± 10.3%, n = 5, $P > 0.99$ vs. MPP^+, Figure 6E). In addition, we found that inclusion of 100 μM cAMP and phosphodiesterase inhibitor IBMX (1 mM) in patch pipette solution was also ineffective in preventing MPP^+-dependent I_h inhibition (47.45 ± 7%, n = 4, $P > 0.99$ vs. MPP^+, Figure 6F). P-values for pharmacology experiments were calculated with one-way ANOVA followed by Bonferroni *post hoc* analysis.

MPP^+ increases temporal summation of EPSPs at STN-SNc glutamatergic synapse

Dendritic I_h prevents or dampens somatic temporal summation at CA3-CA1 synapse by normalizing the amplitude of eEPSPs at the soma (Magee, 1999). Pharmacological blockade of this conductance leads to temporal summation of eEPSPs and, thus, to increased spike probability and overall network excitability. Increased excitatory input has been linked to death from excitotoxicity in several pathological conditions. The SNc receives glutamatergic afferents from the STN and this axonal pathway is preserved in horizontal midbrain slices. We measured synaptic summation of eEPSPs in SNc DA neurons by delivering short trains of low frequency (train duration = 240 ms, frequency = 20 Hz) pulses in the STN. No alteration of synaptic efficacy was ever observed under these conditions. Bath application of 50 μM MPP^+ led to a significant increase of somatic temporal summation, measured as eEPSP 5/eEPSP 1 ratio, from 1.69 ± 0.14 to 2.04 ± 0.13 (n = 9, P = 0.0001) in 9/14 neurons tested. In these neurons, subsequent application of the specific I_h blocker ZD7288 (30 μM) resulted in an additional increase of eEPSP 5/eEPSP 1 ratio from 2.04 ± 0.13 to 2.33 ± 0.13 (n = 9, P = 0.037, Figure 7A, B). In the remaining five neurons, in which MPP^+ did not affect synaptic summation, ZD7288 was also ineffective (P = 0.47, n = 5), thus suggesting that I_h, although detected with somatic current recordings, did not exert a role in synaptic summation. For this reason, ZD7288-irresponsive neurons were excluded by statistical analysis. We applied the same experimental procedure to the CA3-CA1 synapse in hippocampal slices obtained from the same brains (Figure 7A, right), where ZD7288-induced enhancement of temporal summation has been well described (Magee, 1999). Here, no alteration of synaptic summation was observed in response to bath application of MPP^+(1.18 ± 0.08 vs. 1.19 ± 0.1, n = 7, P = 0.99), whereas ZD7288 increased summation significantly (1.19 ± 0.1 vs. 1.85 ± 0.1, n = 7, P = 0.048) in all neurons tested. During eEPSP recordings in both areas, I_h amplitude was measured with single pulses to −75 mV (4 s, holding = −55 mV in SNc, −65 mV in hippocampus) in order to monitor the effectiveness of MPP^+ block. Interestingly, while the increase in temporal summation caused by MPP^+ was always associated to I_h inhibition in the SNc, in the hippocampus, I_h inhibition and increase in somatic summation only occurred with ZD7288, suggesting the existence of differential sensitivity towards MPP^+ among SNc- and CA1-specific hyperpolarization-activated cyclic nucleotide-gated (HCN) isoforms. P-values in eEPSP summation experiments were obtained with one-way ANOVA for repeated measures followed by Bonferroni *post hoc* analysis.

Discussion and conclusions

Micromolar concentrations of MPP^+ affect membrane potential and spontaneous activity through inhibition of I_h

I_h is a non-inactivating, inward-rectifying, cationic current, found in the heart and in many brain areas (Biel *et al.*, 2009). I_h is very abundant in SNc DA neurons (Mercuri *et al.*, 1995) where it is considered a signature current, although its precise neuro-physiological significance in this neuronal population is unclear. Four HCN1–4 channel genes have been identified as the molecular correlates of I_h in mammals. SNc DA neurons in both rat and mouse express HCN2, 3 and 4, characterized by relatively slow activation kinetics and strong sensitivity to cAMP levels. On the other hand, CA1 neurons express HCN1 abundantly, resulting in faster activation kinetics and poor sensitivity to cAMP levels (Franz *et al.*, 2000; Notomi and Shigemoto, 2004). During bath applications of MPP^+ 50 μM, we observed a rapid hyperpolarization along with a reduction of the spontaneous firing activity of SNc DA neurons recorded in whole-cell configuration. These effects were previously described with perforated patch recordings (Liss *et al.*, 2005) and linked to the opening of K_{ATP} channels, caused by mitochondrial failure and drop of cellular ATP contents. Our recordings were obtained in presence of 2 mM ATP, therefore K_{ATP} channels are presumably maintained in a closed state. Consistently, glybenclamide did not prevent the effects of MPP^+ (even in cell-attached recordings) further indicating that, in our experimental conditions, they solely reflect I_h blockade. Notably, a rapid reduction of firing rate is also observed in the work by Liss *et al.* (2005) in SNc DA neurons from mice with non-functional K_{ATP} channels, upon application of MPP^+. Indeed, selective block of I_h was shown to slow the firing rate in midbrain DA neurons previously (Seutin *et al.*, 2001; Inyushin *et al.*, 2010), supporting the hypothesis that MPP^+, via inhibition of I_h, can result in reduced firing activity. No major alterations were found in electrophysiological properties at depolarized potentials. This is not surprising as I_h is closed at potentials above −40 mV. At hyperpolarized potentials we expected a reduction on sag amplitude, yet no significant changes were observed. We interpreted this as a result of the increased input resistance. When I_h is inhibited by MPP^+, the membrane, in addition to being more negative at rest, hyperpolarizes more in response to negative current steps, thereby recruiting a larger fraction of HCN channels and overcoming the inhibitory effect of MPP^+. The depolarization after the sag was fitted with a double exponential function. Both time constants showed a trend to increase with MPP^+ as a result of slower kinetics of activation, in

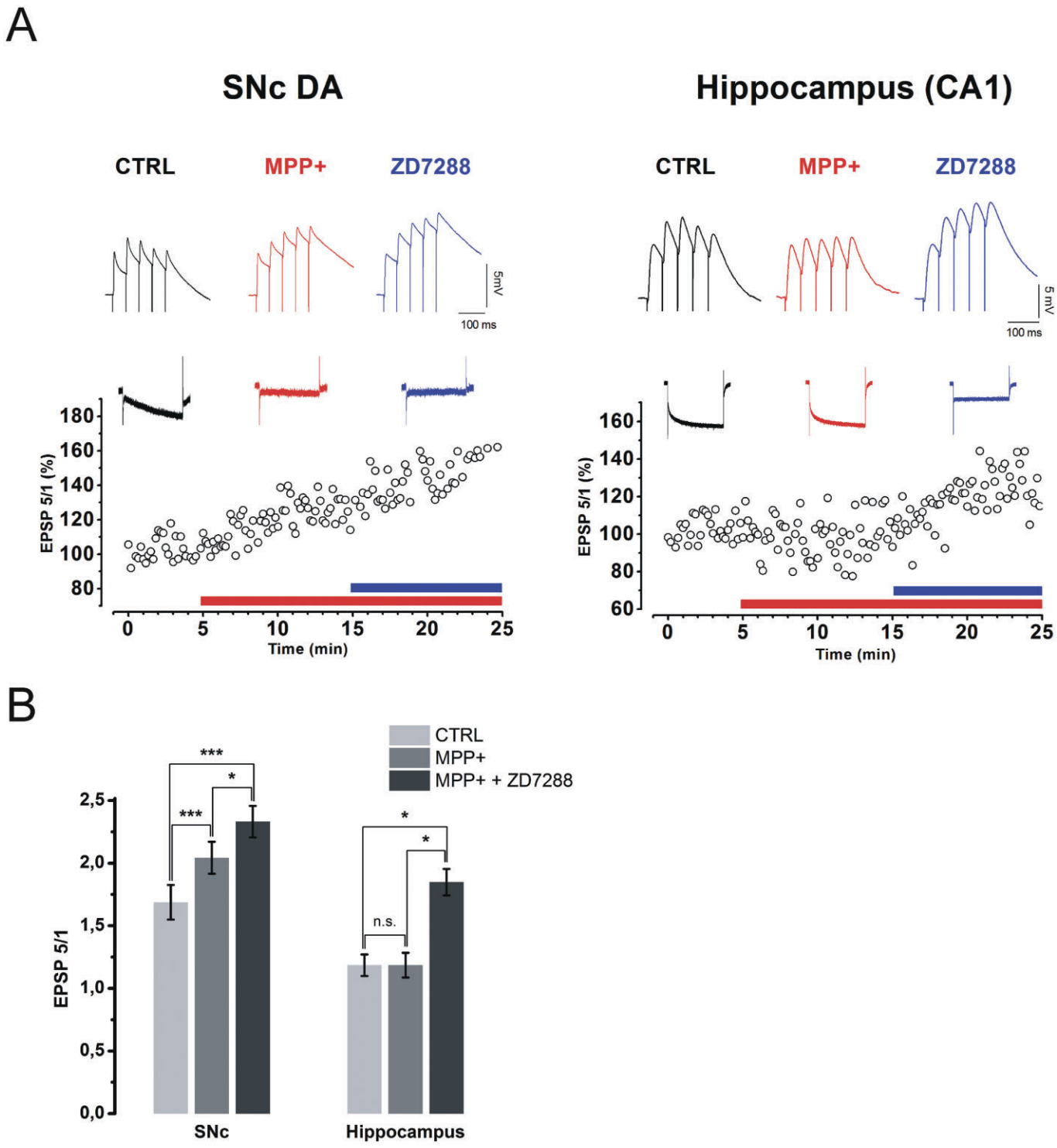

Figure 7

MPP+ enhances temporal summation of eEPSPs in SNc DA, but not in CA1 neurons. (A) Traces showing eEPSP trains in control (black), MPP+ 50 μM (red) and MPP+ 50 μM + ZD7288 30 μM (blue) are shown for representative SNc DA and CA1 hippocampal neurons (Top). Traces were baseline adjusted to allow comparison. The time course of the ratio EPSP 5/EPSP 1 is shown on the bottom. Above each plot, I_h current recordings (step = –75 mV, holding = –55 mV for SNc and –65 mV for CA1) are shown for each condition in the same colour code as for eEPSP examples. (B) eEPSP 5/eEPSP 1 ratio is increase by MPP+ in the SNc (from 1.69 ± 0.14 to 2.04 ± 0.13, $n = 9$, $P = 0.0001$) but not in the hippocampus (from 1.18 ± 0.08 to 1.19 ± 0.1, $n = 7$, $P = 0.99$). ZD7288, as expected, increased summation in CA1 (to 1.85 ± 0.1, $n = 7$, $P = 0.048$) and produced an additional rise in SNc (to 2.33 ± 0.13, $n = 9$, $P = 0.037$). *P*-values were obtained with one-way ANOVA for repeated measures, followed by Bonferroni *post hoc* analysis.

agreement with the effect measured on whole-cell currents (see Table 1).

Biophysical properties of inhibition by MPP$^+$ and pharmacological experiments point to a direct interaction

MPP$^+$-dependent inhibition of I_h was found to be voltage and concentration dependent. A significant shift of the curve towards negative potentials is observed by application of 50 μM MPP$^+$. No differences in this respect were found between juvenile and adult rats or between rats and mice. The shift brought about by MPP$^+$ is not symmetrical, being more evident in the right part of the curve. This does not resemble the effect exerted by cAMP on I_h, as cAMP causes a shift in voltage dependence that is evenly distributed across the activation curve (Biel *et al.*, 2009; Postea and Biel, 2011). MPP$^+$ also produces a substantial slowdown of current activation that is more pronounced at potentials close to rest (–95 mV), consistently with the proximity to values in which inhibition is persistent. During strong and long hyperpolarizing steps (–135 mV, 4 s) MPP$^+$ only affects activation kinetics. Indeed, sustained hyperpolarization (≥3 s) seems to 'rescue' the current so that, at steady state, amplitude reaches control levels. Interestingly, block by ZD7288 is also relieved by prolonged hyperpolarization (Gasparini and DiFrancesco, 1997), although this process unfolds in minutes, compared with few hundred milliseconds for MPP$^+$. These findings concur to suggest a direct interaction of the toxin with the channel. Additional support to this hypothesis has come from the investigation of metabolic and signalling pathways. We first considered whether I_h inhibition could depend on complex I impairment and ensuing ATP depletion/ROS production. As our pipette solution contains ATP 2 mM, depletion of ATP was deemed not influent. The involvement of oxidative stress was tested with rotenone, a complex I blocker previously found to bring about ROS elevation, K_{ATP} channels opening and consequent cessation of firing activity in SNc DA neurons (Liss *et al.*, 2005; Freestone *et al.*, 2009). In our experiments, rotenone left I_h unaffected. Besides, the effect of MPP$^+$ on firing activity and I_h occurred also in presence of the specific K_{ATP} blocker glybenclamide and, in whole-cell recordings, 2 mM ATP. These observations prompted us to look at extramitochondrial mechanisms. The observation that DAT blocker GBR 12783 failed to protect I_h from MPP$^+$- inhibition indicates that the toxin likely acts on the cell surface. Of the many signalling pathways reported to modulate I_h, we focused on those already described in SNc DA neurons. Phosphatidylinositol 4,5-bisphosphate (PIP_2) is a positive modulator of I_h in SNc DA neurons (Zolles *et al.*, 2006). However, block of PIP_2-synthesizing enzyme PI_3 kinase with the specific inhibitor wortmannin leads to the inhibition of I_h in 30 min. As MPP$^+$ is nearly five times faster we discarded the hypothesis of an interaction with this signalling pathway. On the other hand, considering the affinity of MPP$^+$ for DA-specific enzymes and transporters (MAO-B and DAT), we tested the hypothesis that MPP$^+$ could mimic the action of DA on DA receptors, particularly type 2 (D_2R), which are coupled to $G_{i/0}$ proteins. We found that pre-incubation with D_2R antagonist sulpiride was unable to protect I_h from MPP$^+$ inhibitory action. The effect was also not prevented by artificial elevation of intracellular cAMP levels, further indicating that cAMP reduction due to DA-mimicking action of MPP$^+$ on D_2Rs is not relevant here.

MPP$^+$ facilitates temporal summation of eEPSPs in SNc DA neurons via inhibition of I_h

Normalization of EPSPs is afforded by the remarkable distribution of I_h conductance along dendritic arborization found in many neurons (Magee, 1999; Sheets *et al.*, 2011). Thanks to this action, synaptic inputs are conveyed to the soma with temporal precision. This helps avoiding long and potentially noxious depolarizing episodes resulting from temporal summation. When I_h is not functional, due to pharmacological or molecular ablation (Kim *et al.*, 2012), the ability of dendrites to compute and integrate synaptic inputs is lost and robust temporal summation of EPSPs may occur at the soma, leading to greater depolarization and higher firing probability. In the hippocampus and cortex, this promotes the generation of an epileptic focus (Strauss *et al.*, 2004; Jung *et al.*, 2010). Our results suggest that something similar may occur in the SNc in presence of MPP$^+$. Significant elevation of temporal summation of EPSPs originating in STN glutamatergic terminals has been observed during MPP$^+$- and ZD7288-induced block of I_h. Interestingly, MPP$^+$ did not inhibit I_h in CA1 neurons and did not facilitate temporal summation at CA3-CA1 synapse. This supports the conclusion that MPP$^+$ enhances temporal summation in SNc DA neurons through inhibition of I_h and that differential effect may be due to different HCN subunit composition in the two areas.

Relevance to MPP$^+$-induced parkinsonism and PD pathogenesis

We report here that acute inhibition of I_h by MPP$^+$ leads to hyperpolarization, reduction of spontaneous firing activity and increased temporal summation of excitatory inputs in SNc DA neurons. Firing activity of these neurons is very regular *in vitro*, whereas it shows a bursting pattern *in vivo* or in organotypic cultures (Rohrbacher *et al.*, 2000). Given this marked difference, one cannot assume that I_h inhibition by MPP$^+$ reduces discharge frequency of SNc DA neurons *in vivo*. Moreover, a reduction in excitability can hardly be considered noxious in general. Nonetheless, it was reported that the firing activity of SNc DA neurons from adult mice, driven by dendritic voltage-gated calcium channels (Ca_v 1.3), can be reverted to a juvenile specific, I_h-driven firing by pharmacological block of such oscillating calcium conductance (Chan *et al.*, 2007). This phenomenon, named 'rejuvenation' by the authors, was found to be protective *in vitro* and *in vivo*. In this respect, it could be hypothesized that the observed MPP$^+$-dependent suppression of I_h could lead to the inverse process, that is the shift from a 'safe' I_h-driven to a 'noxious' Ca_v 1.3-driven firing pattern, although this would seem rather speculative. On the other hand, the finding that MPP$^+$ enhances synaptic summation of excitatory inputs in SNc DA neurons may have high-potential pathogenic relevance. As reported by studies in many neuronal cells, excessive depolarization due to massive glutamate release (as during ischemia or seizure) results in somatic calcium overload, a major death signal triggering a host of apoptotic pathways (Szydlowska and Tymianski, 2010). In PD, the involvement of

glutamate NMDA receptor is controversial, with some studies showing that NMDA antagonist do not protect from MPTP toxicity (Sonsalla *et al.*, 1992; 1998), and others reporting that impairment of glutamate homeostasis plays a role in this model (Meredith *et al.*, 2009). Regardless of NMDA glutamate receptor involvement, temporal summation leads to greater and more sustained depolarization epochs at the soma and, likely, in dendrites. This may, in turn, result in increased calcium entry through voltage-gated calcium channels. In keeping with this, Surmeier and co-workers have shown that isradipine, a Ca_v 1.3 blocker, is able to stop dendritic calcium oscillations and accumulation and to protect from MPTP-induced degeneration *in vitro* and *in vivo* (Chan *et al.*, 2007; Meredith *et al.*, 2008). Interestingly, it has been reported that I_h is more abundant in calbindin-negative SNc DA neurons and that this subpopulation is more vulnerable in *weaver* and MPTP-lesioned mice (German *et al.*, 1996; Neuhoff *et al.*, 2002). Further studies are required to assess the impact of the functional inactivation of I_h on the viability of SNc DA neurons. Pharmacological or genetic inactivation of I_h in SNc DA neurons in midbrain organotypic cultures or, better, in living animals, will likely reveal whether inhibition of I_h by MPP^+ is a *bona fide* mechanism of toxicity.

Acknowledgements

This work was supported by Regione Toscana Bando salute 2009 (A.M.), the Michael J Fox Foundation for Parkinson's Research RRIA (A.M and G.M.) and Ente Cassa di Risparmio di Firenze (G.M.).

Conflict of interest

With the present document, I declare that none of the authors of this manuscript has any conflict of interest to disclose.

References

Biel M, Wahl-Schott C, Michalakis S, Zong X (2009). Hyperpolarization-activated cation channels: from genes to function. Physiol Rev 89: 847–885.

Blandini F, Armentero MT (2012). Animal models of Parkinson's disease. FEBS J 279: 1156–1166.

Cathala L, Paupardin-Tritsch D (1999). Effect of catecholamines on the hyperpolarization-activated cationic Ih and the inwardly rectifying potassium I(Kir) currents in the rat *substantia nigra pars compacta*. Eur J Neurosci 11: 398–406.

Chan CS, Guzman JN, Ilijic E, Mercer JN, Rick C, Tkatch T *et al.* (2007). 'Rejuvenation' protects neurons in mouse models of Parkinson's disease. Nature 447: 1081–1086.

Choi WS, Kruse SE, Palmiter RD, Xia Z (2008). Mitochondrial complex I inhibition is not required for dopaminergic neuron death induced by rotenone, MPP+, or paraquat. Proc Natl Acad Sci U S A 105: 15136–15141.

Franz O, Liss B, Neu A, Roeper J (2000). Single-cell mRNA expression of HCN1 correlates with a fast gating phenotype of hyperpolarization-activated cyclic nucleotide-gated ion channels (Ih) in central neurons. Eur J Neurosci 12: 2685–2693.

Freestone PS, Chung KK, Guatteo E, Mercuri NB, Nicholson LF, Lipski J (2009). Acute action of rotenone on nigral dopaminergic neurons – involvement of reactive oxygen species and disruption of Ca2+ homeostasis. Eur J Neurosci 30: 1849–1859.

Fuller RW, Hemrick-Luecke SK (1985). Mechanisms of MPTP (1-methyl-4-phenyl-1,2,3,6-tetrahydropyridine) neurotoxicity to striatal dopamine neurons in mice. Prog Neuropsychopharmacol Biol Psychiatry 9: 687–690.

Galvan M, Kupsch A, ten Bruggencate G (1987). Actions of MPTP and MPP+ on synaptic transmission in guinea-pig hippocampal slices. Exp Neurol 96: 289–298.

Gasparini S, DiFrancesco D (1997). Action of the hyperpolarization-activated current (Ih) blocker ZD 7288 in hippocampal CA1 neurons. Pflugers Arch 435: 99–106.

German DC, Nelson EL, Liang CL, Speciale SG, Sinton CM, Sonsalla PK (1996). The neurotoxin MPTP causes degeneration of specific nucleus A8, A9 and A10 dopaminergic neurons in the mouse. Neurodegeneration 5: 299–312.

Greenamyre JT, MacKenzie G, Peng TI, Stephans SE (1999). Mitochondrial dysfunction in Parkinson's disease. Biochem Soc Symp 66: 85–97.

Heikkila RE, Nicklas WJ, Duvoisin RC (1985). Dopaminergic toxicity after the stereotaxic administration of the 1-methyl-4-phenylpyridinium ion (MPP+) to rats. Neurosci Lett 59: 135–140.

Inyushin MU, Arencibia-Albite F, Vazquez-Torres R, Velez-Hernandez ME, Jimenez-Rivera CA (2010). Alpha-2 noradrenergic receptor activation inhibits the hyperpolarization-activated cation current (Ih) in neurons of the ventral tegmental area. Neuroscience 167: 287–297.

Irwin I, Langston JW (1985). Selective accumulation of MPP+ in the substantia nigra: a key to neurotoxicity? Life Sci 36: 207–212.

Jackson-Lewis V, Przedborski S (2007). Protocol for the MPTP mouse model of Parkinson's disease. Nat Protoc 2: 141–151.

Jiang ZG, Pessia M, North RA (1993). Dopamine and baclofen inhibit the hyperpolarization-activated cation current in rat ventral tegmental neurones. J Physiol 462: 753–764.

Jung S, Bullis JB, Lau IH, Jones TD, Warner LN, Poolos NP (2010). Downregulation of dendritic HCN channel gating in epilepsy is mediated by altered phosphorylation signaling. J Neurosci 30: 6678–6688.

Kilkenny C, Browne W, Cuthill IC, Emerson M, Altman DG (2010). NC3Rs Reporting Guidelines Working Group. Br J Pharmacol 160: 1577–1579.

Kim CS, Chang PY, Johnston D (2012). Enhancement of dorsal hippocampal activity by knockdown of HCN1 channels leads to anxiolytic- and antidepressant-like behaviors. Neuron 75: 503–516.

Lacey MG, Mercuri NB, North RA (1987). Dopamine acts on D2 receptors to increase potassium conductance in neurones of the rat substantia nigra zona compacta. J Physiol 392: 397–416.

Lee CY, Lee CH, Shih CC, Liou HH (2008). Paraquat inhibits postsynaptic AMPA receptors on dopaminergic neurons in the substantia nigra pars compacta. Biochem Pharmacol 76: 1155–1164.

Lin AM, Wu LY, Hung KC, Huang HJ, Lei YP, Lu WC *et al.* (2012). Neuroprotective effects of longan (*Dimocarpus longan* Lour.) flower water extract on MPP(+)-induced neurotoxicity in rat brain. J Agric Food Chem 60: 9188–9194.

Liss B, Haeckel O, Wildmann J, Miki T, Seino S, Roeper J (2005). K-ATP channels promote the differential degeneration of dopaminergic midbrain neurons. Nat Neurosci 8: 1742–1751.

Magee JC (1999). Dendritic Ih normalizes temporal summation in hippocampal CA1 neurons. Nat Neurosci 2: 1–13.

McGrath J, Drummond G, McLachlan E, Kilkenny C, Wainwright C (2010). Guidelines for reporting experiments involving animals: the ARRIVE guidelines. Br J Pharmacol 160: 1573–1576.

Mercuri NB, Bonci A, Calabresi P, Stefani A, Bernardi G (1995). Properties of the hyperpolarization-activated cation current Ih in rat midbrain dopaminergic neurons. Eur J Neurosci 7: 462–469.

Meredith GE, Totterdell S, Potashkin JA, Surmeier DJ (2008). Modeling PD pathogenesis in mice: advantages of a chronic MPTP protocol. Parkinsonism Relat Disord 14 (Suppl. 2): S112–S115.

Meredith GE, Totterdell S, Beales M, Meshul CK (2009). Impaired glutamate homeostasis and programmed cell death in a chronic MPTP mouse model of Parkinson's disease. Exp Neurol 219: 334–340.

Neuhoff H, Neu A, Liss B, Roeper J (2002). I(h) channels contribute to the different functional properties of identified dopaminergic subpopulations in the midbrain. J Neurosci 22: 1290–1302.

Notomi T, Shigemoto R (2004). Immunohistochemical localization of Ih channel subunits, HCN1-4, in the rat brain. J Comp Neurol 471: 241–276.

Postea O, Biel M (2011). Exploring HCN channels as novel drug targets. Nat Rev Drug Discov 10: 903–914.

Rohrbacher J, Ichinohe N, Kitai ST (2000). Electrophysiological characteristics of substantia nigra neurons in organotypic cultures: spontaneous and evoked activities. Neuroscience 97: 703–714.

Seutin V, Massotte L, Renette MF, Dresse A (2001). Evidence for a modulatory role of Ih on the firing of a subgroup of midbrain dopamine neurons. Neuroreport 12: 255–258.

Sheets PL, Suter BA, Kiritani T, Chan CS, Surmeier DJ, Shepherd GM (2011). Corticospinal-specific HCN expression in mouse motor cortex: Ih-dependent synaptic integration as a candidate microcircuit mechanism involved in motor control. J Neurophysiol 106: 2216–2231.

Smeyne RJ, Jackson-Lewis V (2005). The MPTP model of Parkinson's disease. Brain Res Mol Brain Res 134: 57–66.

Sonsalla PK, Zeevalk GD, Manzino L, Giovanni A, Nicklas WJ (1992). MK-801 fails to protect against the dopaminergic neuropathology produced by systemic 1-methyl-4-phenyl-1,2,3,6-tetrahydropyridine in mice or intranigral 1-methyl-4-phenylpyridinium in rats. J Neurochem 58: 1979–1982.

Sonsalla PK, Albers DS, Zeevalk GD (1998). Role of glutamate in neurodegeneration of dopamine neurons in several animal models of parkinsonism. Amino Acids 14: 69–74.

Strauss U, Kole MH, Brauer AU, Pahnke J, Bajorat R, Rolfs A *et al.* (2004). An impaired neocortical Ih is associated with enhanced excitability and absence epilepsy. Eur J Neurosci 19: 3048–3058.

Szydlowska K, Tymianski M (2010). Calcium, ischemia and excitotoxicity. Cell Calcium 47: 122–129.

Vargas G, Lucero MT (1999). Dopamine modulates inwardly rectifying hyperpolarization-activated current (Ih) in cultured rat olfactory receptor neurons. J Neurophysiol 81: 149–158.

Zolles G, Klocker N, Wenzel D, Weisser-Thomas J, Fleischmann BK, Roeper J *et al.* (2006). Pacemaking by HCN channels requires interaction with phosphoinositides. Neuron 52: 1027–1036.